Direct numerical analysis of historical structures represented by point clouds

László Kudela*[1], Stefan Kollmannsberger[1], Umut Almac[2], and Ernst Rank[1,3]

[1]Chair for Computation in Engineering, Technische Universität München, Arcisstr. 21, 80333 München, Germany
[2]Istanbul Technical University, Faculty of Architecture, Turkey
[3]Institute for Advanced Study, Technische Universität München, Germany

Abstract

An important field in cultural heritage preservation is the study of the mechanical behavior of historical structures. As there are no computer models available for these objects, the corresponding simulation models are usually derived from point clouds that are recorded by means of digital shape measurement techniques. This contribution demonstrates a method that allows for the direct numerical analysis of structures represented by point clouds. In contrast to standard measurement-to-analysis techniques, the method does not require the recovery of a geometric model or the generation of a boundary conforming finite element mesh. This allows for significant simplifications in the complete analysis procedure. We demonstrate by a numerical example how the method can be used to compute mechanical stresses in a historical building.

1 Introduction

In the past decade, there has been a growing attention towards three-dimensional shape measurement techniques in the context of cultural heritage (CH) preservation. The low cost of equipments and the increasing efficiency and accuracy of the related software have made it possible to create highly detailed 3D, or even 5D digital content of objects both in small and large scales. These digital models are employed in a wide variety of CH related fields, such as documentation, digital restoration, visualization or structural analysis [1, 2, 3]. The latter is particularly important in order to prevent structural failure and to aid the planning of restoration works of damaged structures. In these cases, precise knowledge is needed about the mechanical stresses present in the object.

The most popular technology in engineering for analyzing the stress state of mechanical parts is the Finite Element Method (FEM). It can handle almost arbitrarily complex geometries and topologies which makes the method especially well-suited for the analysis of objects known in the CH context. In standard engineering applications, the FEM model of an object is derived directly from digital plans, e.g. CAD models. However, for many historical structures, there are no digital models available. Moreover, even if there are schematic drawings, the shape of the object may differ from them, especially when the structure is exposed to damaging effects, such as erosion, floods, earthquakes or wars. To overcome this issue, a bridge between shape measurement techniques and the FEM is needed.

Past years' research efforts towards establishing the above link brought forth numerous approaches. Generally, the main steps of such measurement-to-analysis pipelines can be characterized as follows:

*laszlo.kudela@tum.de, Corresponding Author

1. *Data acquisition*
   A 3D shape measurement technique is employed to capture the shape of the domain of interest. This step usually provides a discrete sampling of the surface of the structure, consisting of a large set of points, usually referred to as *point clouds*.

2. *Geometry recovery*
   A geometric model is derived from the point cloud information using geometric segmentation and surface fitting methods. The resulting geometric model is stored using standardized geometric representation techniques, such as STL, STEP or IGES files.

3. *Mesh generation*
   The CAD model from the previous step is discretized into a set of finite elements, commonly referred to as *mesh*.

4. *Finite Element Analysis*
   The mesh is handed over to a finite element solver together with the corresponding material properties and structural constraints.

There are numerous applications that implement the above steps in the context of the structural analysis of CH objects, such as statues [4, 5], masonry arches [6], and historical buildings [7, 8].

An extensive overview of *data acquisition* techniques for CH applications can be found in [9]. The most popular methods are based either on laser scanning, such as in the famous *digital Michelangelo project* [10], or photogrammetric methods, as in [11, 12]. There are applications that aim at combining the advantages of laser scanning and photogrammetry, e.g. the approach in [4].

As for the second step, most approaches convert the point clouds into a surface triangulation by using surface recovery techniques, such as [13, 14]. Because triangulations lack the approximation power to reproduce smooth and curved surfaces efficiently, many applications transform the model further into a more advanced geometric representation format, usually based on non-uniform rational B-splines (NURBS) [15]. These cloud-to-mesh algorithms are implemented in open source tools [16, 17] as well as commercial products, such as Polyworks or Geomagic Studio.

Although there are many open source and commercial meshing solutions available for the third step, it still poses a severe bottleneck in the complete analysis process. Even in standard engineering practice, where geometric models are readily available, the process of mesh generation requires a great amount of human interaction, and may take up to 80% of the total labor time of an engineer [18].

Clearly, the steps of the measurement-to-analysis pipeline are difficult to automate, as a solution which is tailored to a specific class of geometries may not be directly applicable on other types of objects. Furthermore, as the steps require the interplay of methods ranging from point cloud processing to finite element mesh generation, the analyst performing the structural analysis needs to be experienced with a wide variety of softwares and be aware of their respective pitfalls.

In recent years, there has been an increasing interest in the computational mechanics community towards methods that ease the transition from a geometric representation to a finite element model. These research efforts have brought forth many promising approaches, such as the Finite Cell Method (FCM), introduced in [19]. The FCM relies on the combination of approaches well-known in computational mechanics: immersed boundary methods [20] and high order finite elements [21]. It promises very accurate results for geometrically complex objects with almost no meshing costs.

In its simplest implementation, the only information that FCM needs from a geometric model is inside-outside state: given a point in space, does this point lie in the structure of interest or not? A wide variety of geometric representations is able to provide such *point membership tests* and have been shown to work well in combination with the FCM.

The aim of this contribution is to show that the measurement-to-analysis pipeline can be drastically simplified by applying the FCM directly on geometries represented by oriented point clouds. It will be shown that these clouds provide the necessary information for point membership tests, rendering the second and third step of the pipeline unnecessary. The proposed method can be conveniently

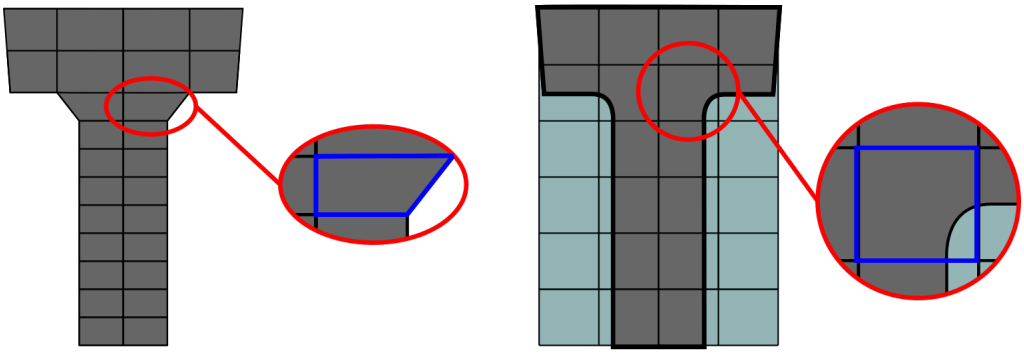

Figure 1: Schematics of the Finite Element (left) and Finite Cell (right) methods. In the FEM, the geometry of interest (gray-colored region) is discretized into a set of boundary-conforming elements. In the FCM, the domain is immersed into a bounding box that contains an extremely soft material, marked with light blue color. The bounding box is subdivided into a regular mesh of quadrilaterals. In contrast to the FEM, finite cell boundaries (dark blue color on the detailed views) do not necessarily conform with the domain boundaries.

applied for the structural analysis of CH objects, which will be demonstrated on a real example of a historical structure.

2 Structural analysis on point clouds using FCM

In the following, the basic ideas of the FEM and the FCM are summarized. The aim of the discussion is to recall the basic concepts only and avoid complex mathematical expressions and derivations. For a thorough analysis, refer to [22] and [23].

2.1 The Finite Element Method

The FEM is a numerical tool which aids engineers and scientists in gaining insight into physical processes that are governed by Partial Differential Equations (PDEs). These equations provide the mathematical basis to describe e.g. how heat propagates in the walls of a building, sound waves travel in halls, or how structures deform when subjected to external forces. While PDEs can be often solved analytically for simple geometries (planar walls, box-like rooms, rectangular plates), it is often impossible to solve them directly for complex shapes. The FEM seeks to overcome this issue by following a bottom-up approach: it breaks down the problem into elementary pieces that behave according to the governing PDE-s in an *approximate* sense (Figure 1).

When, for example, an elementary piece – element – is subjected to a mechanical load, its original shape will undergo a deformation, resulting in a deformed shape. If elementary pieces are carefully assembled together into an interconnected network – mesh –, the individual element deformations together become able to represent the changing shape of the large, more complex-shaped original system.

In the standard, linear version of the FEM, only simple deformations of elements are possible. For example, a side that is straight in the undeformed setting remains straight also in the deformed configuration, even if the underlying physical laws would dictate otherwise. Due to this restriction, the deformation of the complete structure computed by the FEM is only an approximation of the exact deformation that happens in reality. This *discretizaton error* can be reduced in various ways, for example by *refining* the mesh into smaller elements. It can be shown that as the size of the elements in a mesh decreases, the displacements (and the associated stresses) computed by the FEM

get close – converge – to the true values. The tradeoff is that increasing the number of elements leads to longer computational times.

Another popular strategy for reducing the discretization error is to extend the possible deformation modes of the individual elements, which is, for example the approach taken by high-order finite elements (p-FEM) [21]. In p-FEM applications, straight element edges may deform into non-straight, higher order shapes. This strategy also comes at the expense of a higher computational effort. However, for smooth problems, the results offered by p-FEM are subject to much smaller errors than mesh refinement. On the other hand, mesh refinement is a good choice for non-smooth problems, where rapid variations in the displacement field are expected. These phenomena appear typically in the neighborhood of concave corners or material interfaces.

Obviously, the elements in the mesh need to resolve the boundary of the original object as precise as possible. However, they are only allowed to possess simple geometries like triangles, quadrilaterals, tetrahedra, hexahedra etc... Further, they need to satisfy a set of criteria concerning their shape and connectivity properties. These make finite element mesh generation a difficult and time consuming procedure, even if numerous automatic mesh generation softwares are available.

2.2 The Finite Cell Method

One solution to the problem of mesh generation is offered by the Finite Cell Method. The idea of the FCM is to submerge the physical geometry of interest into a virtual box that is filled with an infinitely soft material, referred to as the *fictitious domain*. As the box has a simple geometry, it can be meshed easily, as depicted in Figure 1. Instead of computing on a mesh that resolves the boundaries of the original, *physical domain*, FCM uses a mesh that resolves the boundaries of the box. In this setting, there are *cut elements* that contain parts from the original domain and the fictitious domain as well. Because the fictitious material is infinitely soft, it does not influence the deformation of the physical domain in these elements. However, the deformation may be too complex to be resolved by a coarse mesh of linear elements. Therefore, FCM employs elements from p-FEM, which provide accurate results with moderate computational costs compared to the standard FEM.

In its simplest implementation, the only information that the FCM requires from a geometric model is the inside-outside state: which parts of a given element belong to the fictitious material and which parts to the physical material? Many geometric representations are able to answer such inside-outside queries and have been successfully applied in combination with the FCM. Examples include voxel models from CT-scans [24], constructive solid geometries [25], boundary representations [26] and STL descriptions [27].

2.3 Point membership tests on oriented point clouds

As explained in the introduction, many CH applications that follow the measurement-to-analysis pipeline start from point clouds that represent the structure of interest. Often, the points $\mathbf{p}_i$ in the cloud are equipped with normal vectors $\mathbf{n}_i$, which determine how the local tangent plane of the underlying surface is oriented. The idea is depicted in Figure 2.

This implies a very simple approach for point membership classification:

1. Given a query point $\mathbf{q}$, find the point $\mathbf{p}$ and its associated normal $\mathbf{n}$ in the cloud that lies the closest to $\mathbf{q}$. The two values $\mathbf{p}$ and $\mathbf{n}$ define the local tangent plane of the geometry.

2. Determine the side of the tangent plane on which $\mathbf{q}$ lies, by evaluating the following the scalar product:
$$(\mathbf{p} - \mathbf{q}) \cdot \mathbf{n} \tag{1}$$

3. If the value in Equation 1 is greater than 0, the query point $\mathbf{q}$ lies in the domain. Otherwise, it lies outside.

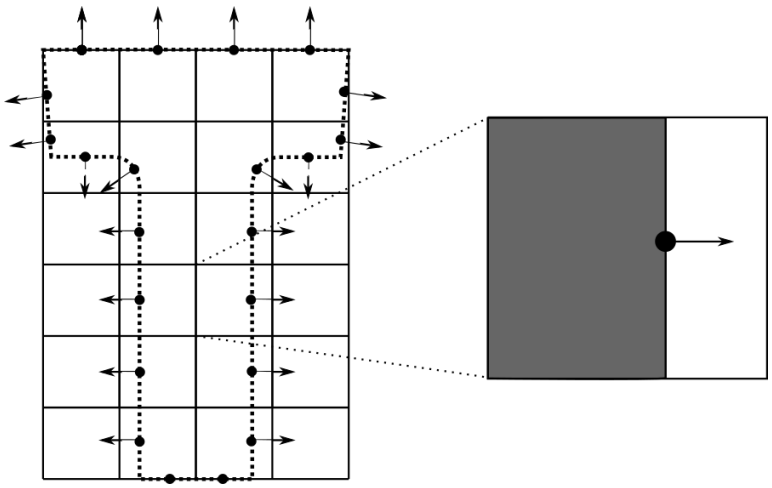

Figure 2: Point membership classification on oriented point clouds. The points and the associated normal vectors represent the local tangent planes of the geometry of interest. They separate the space into physical (gray) and fictitious (white) parts.

The above steps provide the necessary point membership classification needed by the FCM: for any point in any element, it can be decided whether it lies in the physical or the fictitious part of the geometry.

The clouds generated by most scanning procedures are usually not completely clean. They may contain outliers and carry a certain amount of measurement noise, causing the above point membership test to deliver false positives. These effects can be attenuated by performing the test in the k-neighbourhood of the query point. In this process, instead of checking against a single closest point, the k nearest points of $\mathbf{q}$ are found and the point membership with respect to each of them is computed. If $\mathbf{q}$ lies inside with respect to the majority of the points in the k neighborhood, its membership is determined as *inside*, otherwise *outside*. Alternatively, when a greater amount of outliers and noise is present in the cloud, their influence can be reduced by applying cleaning procedures e.g. as in [28].

3 Numerical example: the cistern of the Hagia Thekla Basilica in Turkey

The archaeological site at Hagia Thekla (Meryemlik) was a major pilgrimage site in late antiquity [29]. It was intimately tied to the life of Thekla and her post-mortem miracles. There are numerous structures of different types in the site, which can be identified above ground by sight.

The cistern of the Thekla Basilica is part of the water storage and distribution system of the main church of the site and its sacred area enclosed by walls. It has a rectangular plan measuring approximately 12×14.6 meters in the interior. The interior space is divided into three aisles by two rows of columns (Figures 3 and 4). The columns in each row are connected by arches. Three barrel vaults cover the interior running in the north-south direction.

The columns supporting the upper structure originally had a diameter of approximately 45 cm. They are made of a pink calcareous stone. The columns have double capitals made of limestone. It is not possible to make observations about the condition of the column bases and the floor, due to the thick layer of earth accumulated inside the cistern over centuries. The outer walls are built with a multi-leaf masonry construction system. The outer facing of the walls are made of big limestone blocks, while the inner faces are constructed with brick and mortar. As seen in Figure 4, the cross-sections of the columns have decreased remarkably. The exterior surfaces are flaking due to physicochemical effects; the erosion continues. In addition to surface erosion with a non-uniform pattern, there are deep cavities on the columns. One of the columns (Column 3) has already collapsed

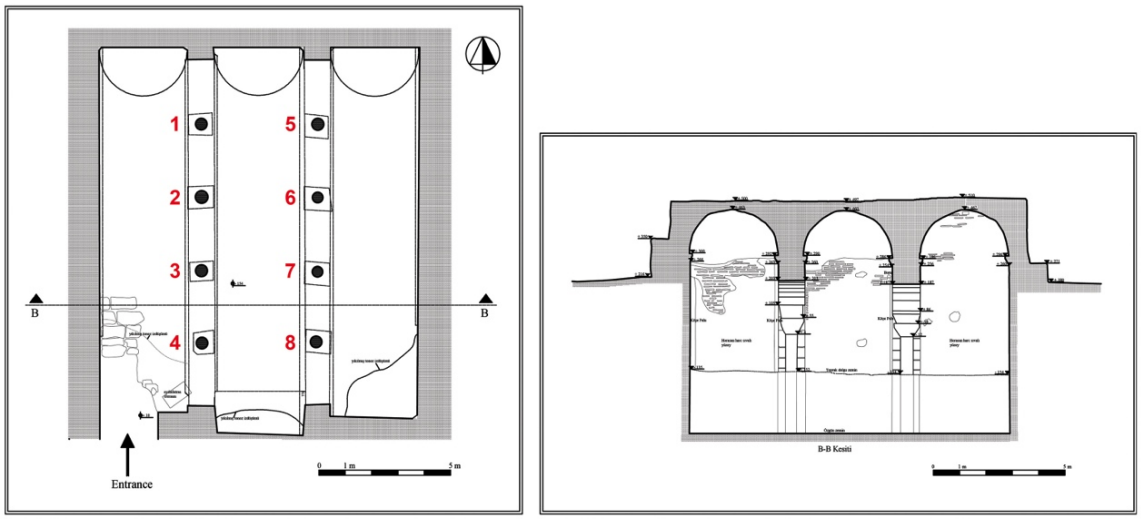

Figure 3: The cistern of Hagia Thekla Basilica, plan and cross section.

Figure 4: A view from the interior of the cistern

and was replaced by a concrete column in the 1960's.

The shape of the decayed column surfaces and cavities are difficult to record using traditional (hand) recording techniques. Therefore, a high definition surveying scanner was employed to document these elements. During the field campaign, the instrument was set up at a number of positions around each column at a distance of a few meters. Thus, overlapping and maximum point density of approx. 5 mm was ensured to represent the highly decayed columns. More details on the measurement process can be found in [7].

3.1 Numerical results computed by the FCM

To examine the stresses throughout the structure under its self weight, a numerical analysis using the FCM was employed. In order to reduce the required computational effort, only one quarter of the structure was investigated. This symmetry reduction is possible because the overall shape of the cystern is symmetric. The point cloud containing columns 5, 6, the voussoir and the supporting wall was immersed in a mesh of 6336 finite cells, as shown in Figure 5.

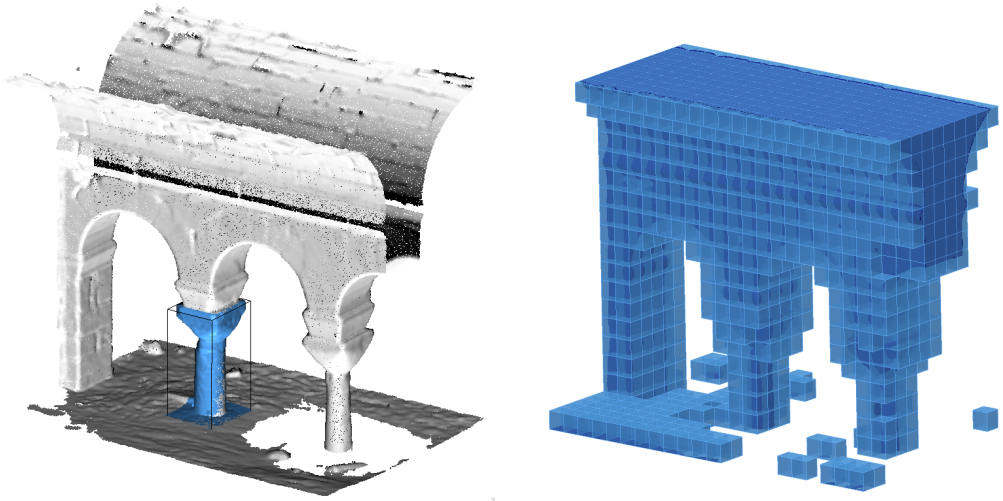

Figure 5: Point cloud representation of the structure of interest and the corresponding mesh of finite cells. Cells that lie completely in the fictitious domain are not plotted.

The most vulnerable elements of the structure are the columns. As stress concentrations are expected at the cavities on the surfaces of the columns, a reduction of the discretization error by mesh refinement is needed. For reasons of efficiency, it is important to refine the mesh only around the columns, where the stress field is expected to change rapidly. For the FEM and the FCM, such *local refinement* techniques have been well-studied recently. In our applications, we employ the *multi-level hp-adaptivity* technique of [30]. In the refinement procedure, those cells that are intersected by the points representing column 5 (the blue points on Figure 5) are recursively subdivided into eight equal subcells, until a subdivision depth of 5 is reached. A cross sectional view of the refined mesh is depicted in Figure 6.

The material properties were defined to be linear elastic and isotropic, with an elastic modulus and Poisson's ratio of $E = 2 \cdot 10^4$MPa and $\nu = 0.2$, respectively. The specific gravity of the material was set to 27 kN/m^3. In the fictitious domain, the material was given a stiffness of 2 MPa. The foundation of the structure was rigidly fixed to the ground.

The maximum principal stress distribution computed by the FCM is depicted in Figure 7. As expected, the highest compressive stresses occur in the columns. The stress values are in the range of 2..4 MPa, while the peak value occurs at the connection between the column and the capital. This is in good agreement with the values computed in [7], following the traditional measurement-to-analysis procedure.

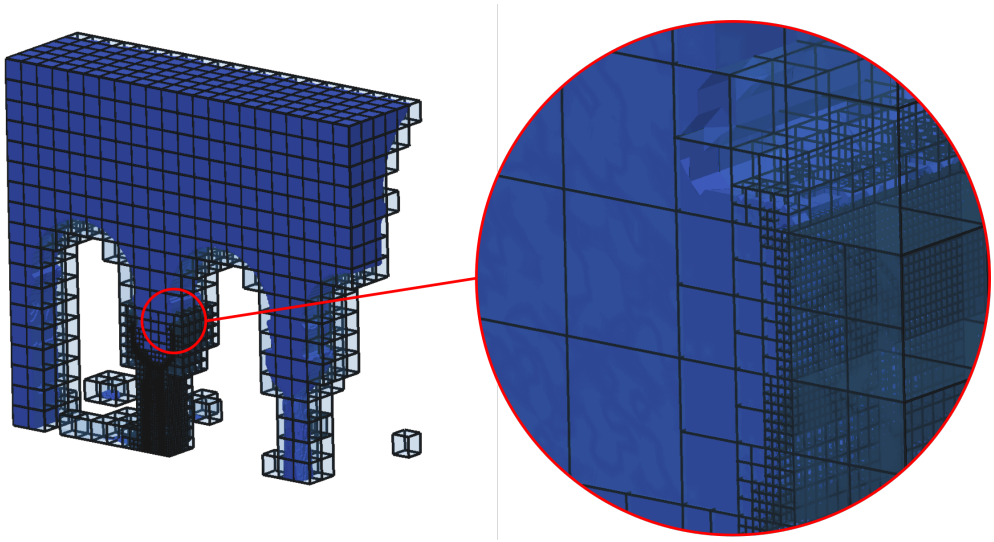

Figure 6: Locally refined finite cell mesh. The cells around the column of interest are recursively subdivided towards the geometric boundary.

4 Conclusions

This contribution presented a technique that aims at the direct structural analysis of CH structures represented by oriented point clouds. The approach is based on the Finite Cell Method, which, in its simplest implementation, only requires inside-outside information from the geometric model of interest. It was shown that oriented point clouds are able to provide such point membership tests. In contrast to standard approaches, the proposed technique does not need the recovery of a geometric model or the generation of a boundary conforming finite element mesh. This allows for significant simplifications in the measurement-to-analysis pipeline, establishing a seamless connection between shape measurement techniques and numerical simulations. A numerical example demonstrated that the method can be conveniently applied for the structural analysis of historical structures.

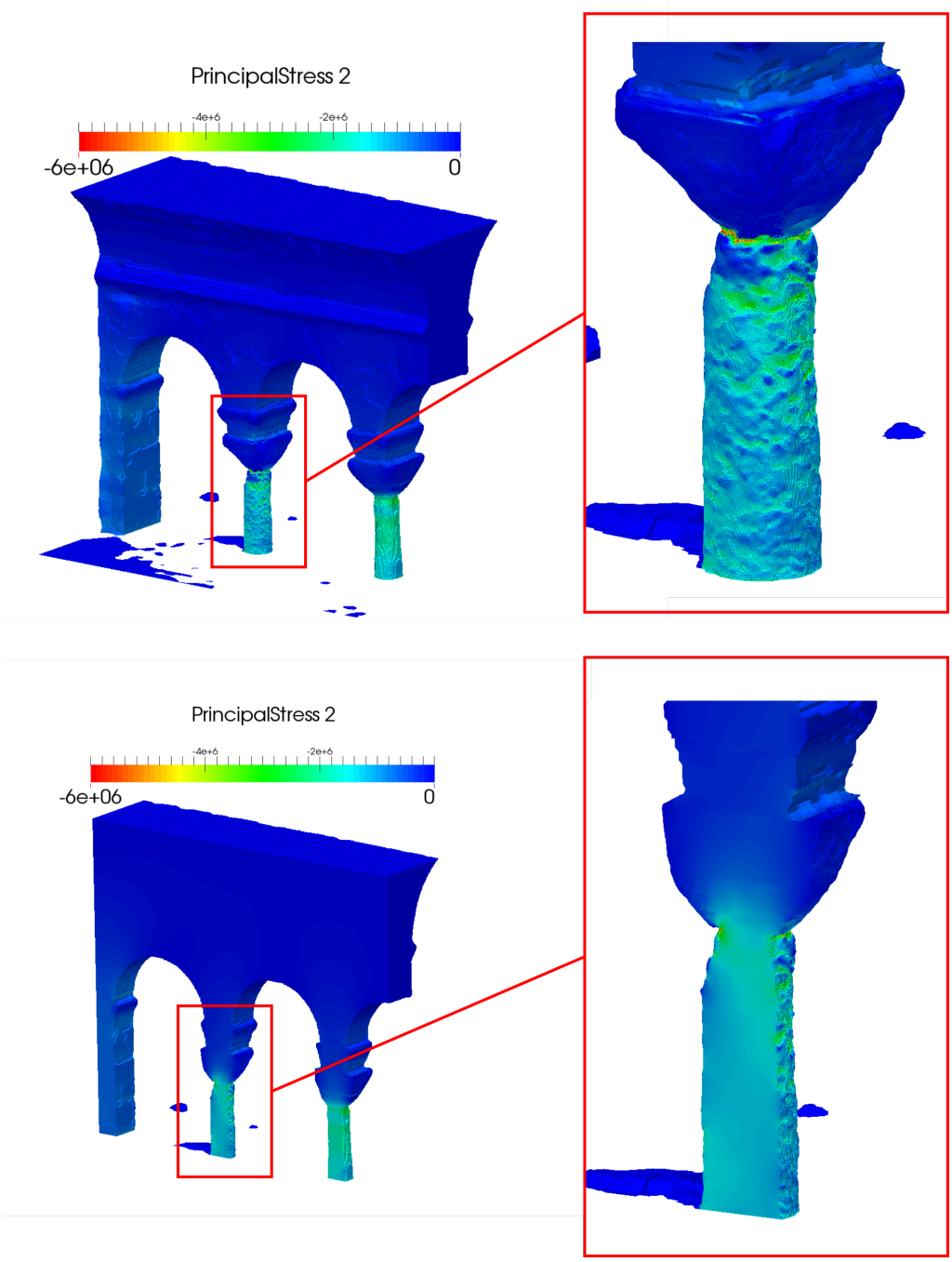

Figure 7: Maximum principal stress distribution computed by the FCM, with a detailed view over column no. 6. Top: the stress field on the surface. Bottom: internal stresses along a cross-section. The values are in Pa.

References

[1] Fabio Bruno, Stefano Bruno, Giovanna De Sensi, Maria-Laura Luchi, Stefania Mancuso, and Maurizio Muzzupappa. From 3D reconstruction to virtual reality: A complete methodology for digital archaeological exhibition. *Journal of Cultural Heritage*, 11(1):42–49, 2010.

[2] Filippo Stanco, Sebastiano Battiato, and Giovanni Gallo. *Digital imaging for cultural heritage preservation: Analysis, restoration, and reconstruction of ancient artworks*. CRC Press, 2011.

[3] Anastasios Doulamis, Nikolaos Doulamis, Charalabos Ioannidis, Christina Chrysouli, Nikos Grammalidis, Kosmas Dimitropoulos, Chryssy Potsiou, Elisavet Konstantina Stathopoulou, and Marinos Ioannides. 5d modelling: An efficient approach for creating spatiotemporal predictive 3d maps of large-scale cultural resources. *ISPRS Annals of Photogrammetry, Remote Sensing & Spatial Information Sciences*, 2015.

[4] Ilias Kalisperakis, Christos Stentoumis, Lazaros Grammatikopoulos, Maria Eleni Dasiou, and Ioannis N Psycharis. Precise 3d recording for finite element analysis. In *Digital Heritage, 2015*, volume 2, pages 121–124. IEEE, 2015.

[5] Andrea Borri and Andrea Grazini. Diagnostic analysis of the lesions and stability of Michelangelo's David. *Journal of Cultural Heritage*, 7(4):273–285, 2006.

[6] B Riveiro, JC Caamaño, P Arias, and E Sanz. Photogrammetric 3D modelling and mechanical analysis of masonry arches: An approach based on a discontinuous model of voussoirs. *Automation in Construction*, 20(4):380–388, 2011.

[7] Umut Almac, Isıl Polat Pekmezci, and Metin Ahunbay. Numerical Analysis of Historic Structural Elements Using 3D Point Cloud Data. *The Open Construction and Building Technology Journal*, 10(1), 2016.

[8] Giovanni Castellazzi, Antonio Maria D'Altri, Gabriele Bitelli, Ilenia Selvaggi, and Alessandro Lambertini. From laser scanning to finite element analysis of complex buildings by using a semi-automatic procedure. *Sensors*, 15(8):18360–18380, 2015.

[9] George Pavlidis, Anestis Koutsoudis, Fotis Arnaoutoglou, Vassilios Tsioukas, and Christodoulos Chamzas. Methods for 3d digitization of cultural heritage. *Journal of cultural heritage*, 8(1):93–98, 2007.

[10] Marc Levoy, Kari Pulli, Brian Curless, Szymon Rusinkiewicz, David Koller, Lucas Pereira, Matt Ginzton, Sean Anderson, James Davis, Jeremy Ginsberg, et al. The digital Michelangelo project: 3D scanning of large statues. In *Proceedings of the 27th annual conference on Computer graphics and interactive techniques*, pages 131–144. ACM Press/Addison-Wesley Publishing Co., 2000.

[11] Sameer Agarwal, Yasutaka Furukawa, Noah Snavely, Ian Simon, Brian Curless, Steven M Seitz, and Richard Szeliski. Building rome in a day. *Communications of the ACM*, 54(10):105–112, 2011.

[12] Maurizio Muzzupappa, Alessandro Gallo, Francesco Spadafora, Felix Manfredi, Fabio Bruno, and Antonio Lamarca. 3D reconstruction of an outdoor archaeological site through a multi-view stereo technique. In *Digital Heritage International Congress (DigitalHeritage), 2013*, volume 1, pages 169–176. IEEE, 2013.

[13] Michael Kazhdan and Hugues Hoppe. Screened poisson surface reconstruction. *ACM Transactions on Graphics (ToG)*, 32(3):29, 2013.

[14] Fatih Calakli and Gabriel Taubin. Ssd: Smooth signed distance surface reconstruction. In *Computer Graphics Forum*, volume 30, pages 1993–2002. Wiley Online Library, 2011.

[15] Les Piegl and Wayne Tiller. *The NURBS book*. Springer Science & Business Media, 2012.

[16] Paolo Cignoni, Marco Callieri, Massimiliano Corsini, Matteo Dellepiane, Fabio Ganovelli, and Guido Ranzuglia. Meshlab: an open-source mesh processing tool. In *Eurographics Italian Chapter Conference*, volume 2008, pages 129–136, 2008.

[17] Radu Bogdan Rusu and Steve Cousins. 3D is here: Point Cloud Library (PCL). In *IEEE International Conference on Robotics and Automation (ICRA)*, Shanghai, China, May 9-13 2011.

[18] J Austin Cottrell, Thomas JR Hughes, and Yuri Bazilevs. *Isogeometric analysis: toward integration of CAD and FEA*. John Wiley & Sons, 2009.

[19] Jamshid Parvizian, Alexander Düster, and Ernst Rank. Finite cell method. *Computational Mechanics*, 41(1):121–133, 2007.

[20] Charles S Peskin. The immersed boundary method. *Acta numerica*, 11:479–517, 2002.

[21] Barna Szabó, Alexander Düster, and Ernst Rank. The p-version of the finite element method. *Encyclopedia of computational mechanics*, 2004.

[22] Olgierd Cecil Zienkiewicz, Robert Leroy Taylor, Olgierd Cecil Zienkiewicz, and Robert Lee Taylor. *The finite element method*, volume 3. McGraw-hill London, 1977.

[23] Alexander Düster, Ernst Rank, and Barna Szabó. The p-Version of the Finite Element and Finite Cell Methods. *Encyclopedia of Computational Mechanics Second Edition*, 2017.

[24] Martin Ruess, David Tal, Nir Trabelsi, Zohar Yosibash, and Ernst Rank. The finite cell method for bone simulations: verification and validation. *Biomechanics and modeling in mechanobiology*, 11(3-4):425–437, 2012.

[25] Benjamin Wassermann, Stefan Kollmannsberger, Tino Bog, and Ernst Rank. From geometric design to numerical analysis: A direct approach using the Finite Cell Method on Constructive Solid Geometry. *Computers & Mathematics with Applications*, 74(7):1703–1726, 2017.

[26] László Kudela, Nils Zander, Stefan Kollmannsberger, and Ernst Rank. Smart octrees: Accurately integrating discontinuous functions in 3D. *Computer Methods in Applied Mechanics and Engineering*, 306:406–426, 2016.

[27] Mohamed Elhaddad, Nils Zander, Stefan Kollmannsberger, Ali Shadavakhsh, Vera Nübel, and Ernst Rank. Finite Cell Method: High-Order Structural Dynamics for Complex Geometries. *International Journal of Structural Stability and Dynamics*, page 1540018, 2015.

[28] Oliver Schall, Alexander Belyaev, and H-P Seidel. Robust filtering of noisy scattered point data. In *Point-Based Graphics, 2005. Eurographics/IEEE VGTC Symposium Proceedings*, pages 71–144. IEEE, 2005.

[29] Stephen Hill. *The early Byzantine churches of Cilicia and Isauria*. Variorum Aldershot, UK, 1996.

[30] Nils Zander, Tino Bog, Stefan Kollmannsberger, Dominik Schillinger, and Ernst Rank. Multi-level hp-adaptivity: high-order mesh adaptivity without the difficulties of constraining hanging nodes. *Computational Mechanics*, 55(3):499–517, 2015.